



Research Article

High Performance Conductive Composites and E-skins with Large-scale Manufacturing for Wearable Electronic Sensor Systems

R Madhavan^{1*}

¹Department of Science, Technology, and Engineering, Industrial Production and Processing Facility

*Correspondence to: R Madhavan, PhD, Full-Professor, Department of Science, Technology, and Engineering, Industrial Production and Processing Facility; E-mail: madhavan_rajaa@rediffmail.com

Received: August 2, 2024 Revised: September 13, 2024 Accepted: October 18, 2024 Published: November 21, 2024

Abstract

Objective: High performance wearable sensors for biological and bio-technological recognition of human epidermal movements and muscle tissue deformations are attracting widespread attention and demonstrate fascinating potential for future wearable electronics.

Methods: This work demonstrates conductive networks and film cracks-based stretchable strain sensors using carbonic sensing layers / mold star silicone elastomer nanocomposites.

Results: The as-fabricated stretchable strain sensors demonstrate captivating superiority, including simplicity in the fabrication steps and ultra-high strain sensitivity far exceeding recently reported state-of-the-art strain sensors. Prominently, the stretchable strain sensors exhibit dazzling piezoresistivity with a high gauge factor of 2,185 and a wide sensing range of 30% strain. The working mechanism depends on the electrical resistance variations, which is strikingly altered by a percolating network crack surface microstructure due to strain concentration during tensile deformations. The ultra-sensitive sensing performance in conjunction with a wide sensing range, prominent linearity ($R^2 > 0.99$ in the strain range of 15-30%), excellent reversibility characteristics and remarkable durability (more than 1,300 stretch-release cycles under a large-scale strain of 30%) for large-scale tensile deformations.

Conclusion: The stretchable strain sensors to be employed as wearable strain monitoring devices for the diverse-range of practical applications, including but not confined to multi-scale monitoring, electronic skins, smart robotics, human-machine / computer interfaces, as well as sports performance monitoring.

Keywords: science, technology and engineering, energy sustainability, biological recognition, biotechnological monitoring, sensor design, flexible electronics, wearable electronics, spray processes, wearable sensors, conductive composites

Citation: Madhavan R. High Performance Conductive Composites and E-skins with Large-scale Manufacturing for Wearable Electronic Sensor Systems. *J Mod Nanotechnol*, 2024; 4: 5. DOI: 10.53964/jmn.2024005.

1 INTRODUCTION

Flexible, stretchable and epidermis-attachable strain sensors, which transduce external strains into efficiently recognizable electronic signals^[1-3], demonstrate broad applications in healthcare monitoring^[1-5], soft robotics^[1-3,6,7], and sport activity recognition^[1-3,8]. Tiny mechanical stimulations generated by pulse wave signals^[9], facial expressions^[10], phonation^[11], and breath monitoring^[12] are detected for health monitoring. On the other hand, large mechanical deformations induced by bending process of a finger, wrist, elbow, and knee joint movements are recorded for sport activity recognition^[1,2,13], biomechanics and kinesiology applications^[1,2,14], human-machine interfaces^[15], virtual reality and entertainment technologies^[16,17]. These applications involve different strain ranges, which in turn require different sensitivities. For instance, high sensitivity (gauge factor>100) is crucial for the monitoring of healthcare signals and extracting quality medical data^[18,19]. On the other hand, for the monitoring of large mechanical deformations induced by human joint motions, low sensitivity (gauge factor<5) is typically sufficient^[20]. Moreover, in stretchable and skin-attachable strain sensors, there exists a substantial trade-off between the strain sensitivity and strain range^[21-24]. In other words, it is still a huge challenge to obtain both a high sensitivity and a broad strain range simultaneously in one versatile stretchable strain sensor. Therefore, fabricating stretchable strain sensors with suitable sensitivity and strain range is of great significance for reliable strain monitoring. Stretchable and skin-attachable strain sensors can be classified as piezoresistive^[25-27], piezocapacitive^[28-30], piezoresistive-piezocapacitive^[31], optical^[32,33], and piezoelectric sensors^[34-36]. Among these, the piezoresistive strain sensors have attracted widespread attention owing to their facile design, friendly readout mechanisms, simple structures, and high sensitivities^[37,38].

The sensitivity of stretchable piezoresistive strain sensors is evaluated through gauge factor (GF)^[18,37,39,40].

$$GF = \frac{\Delta R/R_0}{\varepsilon}$$

where $\Delta R/R_0$ ($= (R - R_0) / R_0$) is the electrical resistance variation with mechanical strain, R_0 is the electrical resistance at an unstrained condition, and ε ($= (L - L_0) / L_0$) is the applied mechanical strain. The stretchable piezoresistive strain sensors are normally comprised of electrically conductive materials including carbon materials (graphite,^[41] carbon nanotubes^[42,43], graphene (Gr)^[11,44,45]) MXenes (e.g. $\text{Ti}_3\text{C}_2\text{T}_x$)^[46,47], metal nanomaterials (nanowires^[14,48,49], and nanoparticles^[50,51]), and ionogels^[52,53] embedded onto flexible/stretchable supporting materials.

Recently, substantial attention is focused on fabricating stretchable and skin-attachable strain sensors based on graphitic carbon conductive materials embedded onto flexible / stretchable supporting materials owing

to their unique electrical performance, and mechanical resilience^[41,54,55]. Other than wearable strain sensors, they have been demonstrated for field effect transistors^[56], memory devices^[57], solar cells^[58,59], energy harvesters^[60,61], and energy storage devices^[62,63]. However, for strain monitoring, it is a grand challenge to achieve high strain sensing performance in terms of strain sensitivity and strain range. For instance, Wu et al. reported a flexible strain sensor based on Graphite nanoplatelets / Polyurethane (PU) nanocomposites with a sensing strain range of up to 30% and a gauge factor of 0.9^[54]. Zhang et al. developed a flexible strain sensor based on Graphite flakes/Silk fiber composites with a strain sensing range of up to 15% and a gauge factor of 14.5, respectively^[55].

Moreover, their fabrication is associated with complexity, involves multiple procedures, and produces environmentally non-friendly wastes in significant quantities. In recent years, fabrication processes involving spray deposition of functional materials onto target substrates have been extensively employed for developing various electronic devices including stretchable and skin-attachable strain sensors^[64,65], pressure sensors^[66,67], organic electrochemical transistors^[68,69], and solar cells^[70,71] owing to their numerous advantages such as cost-effectiveness, high-throughput production, and capability of coating functional materials onto intricate, and curved surfaces in a contactless manner^[72].

In order to achieve high performance in stretchable strain sensors, specifically with regard to the GFs, the mechanical crack generation in the electrically conductive networks is garnering significant research attention. For example, Wang et al. achieved conductive network cracks through the pre-stretching process by utilizing stiffness mismatch between the functional sensor materials and stretchable matrix^[23]. As a result, this strain sensor demonstrated a maximum gauge factor of 87. Liu et al. generated the parallel nanocracks on the elastomer supporting material through an ultrasonication process during the sensor fabrication^[48]. Kang et al. fabricated nanoscale crack-assisted strain gauge sensors through the inspiration of spider sensory system^[73]. Lin et al. fabricated wearable multifunctional sensors based on Rubber / carbon nanotube (CNT) with a gauge factor of up to 25.98^[74].

In recent years, wearable and stretchable strain sensors are garnering tremendous attention for real-life practical sensing applications such as human motion / activity monitoring, human healthcare monitoring, human - machine interfaces, soft robotics and many more exciting applications of practical interest. For example, Wang et al. fabricated foam - shaped stretchable strain sensors based on MXene ($\text{Ti}_3\text{C}_2\text{T}_x$) - multiwalled carbon nanotubes (MWCNTs) / Thermoplastic polyurethane (TPU) nanocomposites via salt - templating and dip - coating processes for the monitoring of human activities^[46].

As a result, the strain sensors demonstrated significant applicability in wearable electronics. Xu et al. developed stretchable and wearable strain sensors based on CNT-Ti₃C₂T_x MXene / Polydimethylsiloxane (PDMS) nanocomposites using vacuum filtration for human motion and healthcare monitoring applications^[5]. Liu et al. fabricated wearable and stretchable strain sensors with high breathability based on copper nanoparticles - viscose yarn / Lycra fabrics via polymer - assisted metal deposition (PAMD) and lock - stitch embroidery^[8]. Han et al. fabricated wearable and stretchable strain sensors based on silver nanowires (AgNWs)-copper nanowires (CuNWs) - CNTs / Ecoflex nanocomposites utilizing drop - casting and spin - coating techniques for human motion and healthcare monitoring, electronic skins, smart robotics, human-machine interfaces^[18]. Wang et al. reported the great benefits of skin - like wearable strain sensors for human machine interfacing applications such as virtual and augmented reality^[17].

Herein, this work presents a high performance stretchable and skin-attachable strain sensor by embedding spray coated carbonic conductive network within two layers of mold star silicone elastomers for detecting entire - range of human body motions for healthcare applications. The as - fabricated strain sensors demonstrate many fascinating merits including ultra - high gauge factor of 2,185, a broad strain range of up to 30%, high linearity ($R^2 > 0.99$ in the strain range of 15-30%), ultra-low limit of monitoring (0.1% strain), and prominent durability (more than 1,300 stretch-release cycles under a large-scale strain of 30%). As skin - attachable strain sensors, real - life sensing applications of detecting and monitoring the human body motions from tiny stimulations to large - scale deformations are demonstrated in this research, which can be of benefit for burgeoning applications in wearable electronics field.

2 EXPERIMENTAL SECTION

2.1 Materials

The Smooth - On, Inc. Mold Star™ - 20T (Part A and Part B) was used as procured. Carbonic sensor materials were obtained from Kontakt Chemie, Ltd. Smooth - On, Inc. Skin-Tite™ (Part A and Part B) kit was purchased for device lamination and on-skin attachability.

2.2 Fabrication of The Stretchable Component

The stretchable Mold Star silicone elastomeric films were obtained by mixing Part A and Part B thoroughly at a mixing ratio of 1A:1B by volume. Next, the thoroughly mixed liquid Mold Star was poured and spread evenly onto a Polyethylene terephthalate (PET) substrate. After that, the curing process was carried out at room temperature for 30min. Once fully cured, the mold star silicone elastomeric films were exfoliated from the PET surface for further processing steps.

2.3 Fabrication of the Wearable Strain Sensors

The stretchable Mold Star silicone elastomeric films were rinsed thoroughly utilizing ethanol. After that, the previously cleaned elastomeric films were fixed firmly onto a rigid support for coating of electrically conductive materials. The carbonic materials were spray coated onto the Mold Star silicone elastomeric films followed by naturally drying in ambient conditions to form highly conductive carbonic conductive networks. Electrical wires were fixed onto both the ends of the electrically conductive film using a fast-drying conductive silver paste. For achieving a stable electro - mechanical performance, sandwich structured strain sensors were fabricated by curing liquid mold star over the carbonic sensing layers / mold star composites, which encapsulates the electrically conductive carbonic film in between the two slabs of mold star silicone elastomeric films.

2.4 Material Characterization

The optical micrographs of carbonic sensing layers / mold star composites at various stretching strains were taken utilizing an optical microscope (Inskam, Inc). A motorized moving stage was utilized for applying stretching-releasing strains onto the wearable strain sensors through gripping the strain sensors using 3M very high bond (VHB) Tape 4,910 and fast - drying cyanoacrylate adhesive for evaluating the electromechanical performance. To demonstrate the multi - scale human motion monitoring ability, the wearable sensors were intimately laminated onto the various locations of the human body utilizing a skin - safe bio - adhesive, Skin - Tite (Smooth - On, Inc). Digital multimeters were utilized to record the electrical signal variations in a real - time fashion during the strain monitoring experiments.

2.5 Flexible Strain Sensor Tests on Human Skin

The flexible strain sensor tests on human skin reported in this work does not require any sort of Institutional Review Board approvals owing to the non-influencing nature of these sensing demonstrations to humans. In addition, the human subject, i.e., author of this article provided his consent to publish his photographs reported in the research data.

2.6 Funding Statement

The independent research is self-funded by the author, Madhavan R (Independent Scientist).

3 RESULTS AND DISCUSSION

Figure 1 illustrates the fabrication strategy of the newly developed straight line - type Mold-star / Carbonic sensing layers (CSLs) / Mold-star nanocomposite-based sandwich structural stretchable strain sensors. The detailed fabrication strategy is illustrated in the experimental section. The Mold-star / CSLs / Mold-star nanocomposite-based sandwich

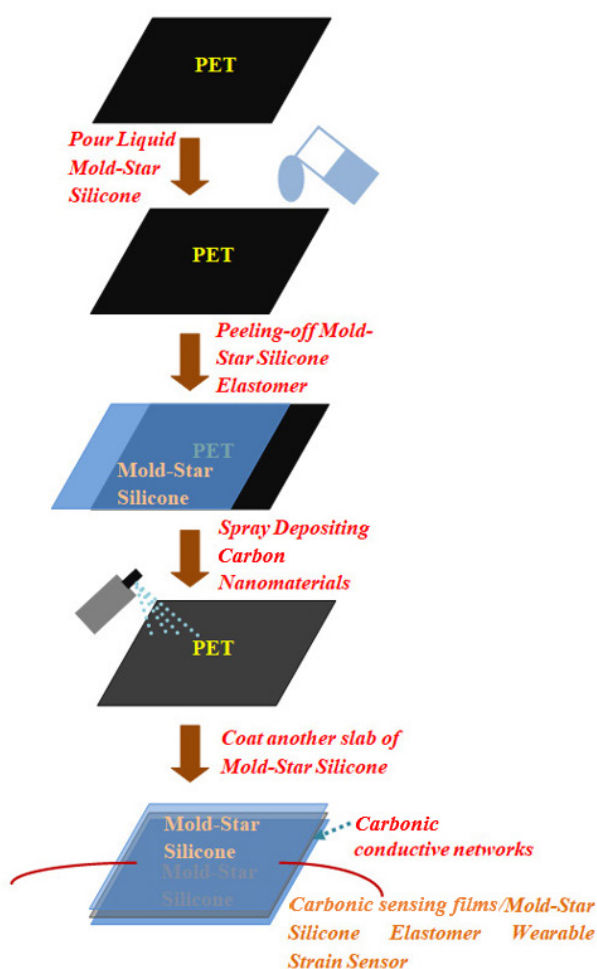


Figure 1. Schematic of the Fabrication Process of the CSLs / Mold-star Nanocomposite-based Strain Sensor.

Pour liquid mold star silicone on PET. Peel off the cured mold star film. Spray deposit the carbon nanomaterials to form the conductive film. Attach electrical wires and coat another layer of mold star silicone for encapsulation.

structural strain sensors developed in this work demonstrate outstanding mechanical resilience as illustrated in Figure 2A and 2B, thereby implying the ability of obtaining stable device performance during the application of multi-scale strains (or deformations). The spray coated sandwich structural strain sensors can be tightly attached onto the human epidermal surfaces as well as onto complex, irregular, and intricate surfaces with negligible damage to the strain sensors owing to their sandwich structured design. The highly uniform spray deposited CSLs film with strong interfacial bonding is shown in Figure 2C via cross-sectional morphology of the sensor. It is worth to mention that, during the dropping process of liquid Mold-star silicones onto the CSLs / Mold-star nanocomposite, the liquid silicones encapsulate (or incorporate) the CSLs owing to their large viscosity. Once fully cured, the CSLs are mechanically interlocked with the Mold-star silicone elastomers, exhibiting fascinating adhesion characteristics, which will be a benefit for achieving reliable and stable strain sensor performance for wearable electronics. This work utilizes novel Mold-star silicone elastomers for the

fabrication of high performance wearable strain sensors owing to their captivating advantages, including, a much higher viscosity than the previously reported stretchable supporting materials (or stretchable substrates) such as Ecoflex, PDMS, and TPU, which provides the strong interfacial bonding between CSLs and Mold-star silicones. In addition, Mold-star is an epidermis-like ultra-soft silicone elastomer with a Young's modulus of 324kPa, delivering crucial mechanical compliance similar to that of human epidermal surfaces, owing to which, the spray coated strain sensors of this work can be efficiently integrated with the human epidermis for the real-time detection and monitoring of human bodily motions / activities, respectively.

3.1 Properties and Performance of Conductive Elastomer Complexes

In this work, a spray coating process is illustrated which will be beneficial for the deposition of carbonic films onto various stretchable supporting materials (or stretchable substrates) typically employed for the development of flexible and stretchable electronic devices (Ecoflex, Dragon skin, Natural rubber, Nitrile rubber, Rebound silicone elastomer, Smooth-Sil, Thermoplastic PUs, and textile fabrics) resulting in high sensitivity and high stretchability simultaneously. The epidermal strain sensors based on Carbonic films / Mold star nanocomposites exhibit a detection limit as low as 0.1% strain and a strain range as high as 30%, simultaneously with highly linear ultrasensitive gauge factor value of 2,185 ($R^2 > 0.99$), fast strain responsiveness and recovery ($< 500\text{ms}$). Moreover, the electronic device demonstrated excellent durability (more than 1,300 cycles at 30% strain) with negligible loading-unloading signal variations over 1,300 stretch-release cycles. The captivating sensing performances enabled monitoring of multi-scale human bodily motions (canthus muscle motion (or eye blinking activities), cheek motions, frowning activity, throat muscle deformation and vocal cord vibrations, bending process of a finger, wrist motion, elbow bending, and knee joint motions) in a real-time scenario. The fabrication process of Carbonic films / Mold star nanocomposite-based strain sensors is schematically illustrated in Figure 1. A mold star silicone elastomer was sandwiched between a flat wooden block and an acrylic mask with a rectangular pattern ($30 \times 5\text{mm}^2$). After that, the carbonic materials were spray deposited onto the open area of acrylic mask with a rectangular (or straight line-type) pattern and dried in ambient conditions. After the removal of wooden block and acrylic mask, conductive carbonic film was achieved with a typical conductivity of $\sim 1\text{k}\Omega$.

The carbonic conductive network fabrication was of a scalable kind, which could be extended to a diverse range of elastic and stretchable supporting materials (Ecoflex, Dragon skin, Natural rubber, Nitrile rubber, Rebound silicone elastomer, Smooth-Sil, Thermoplastic PUs, and textile fabrics) with benefit of strong adhesion and uniform deposition, which could be useful in obtaining

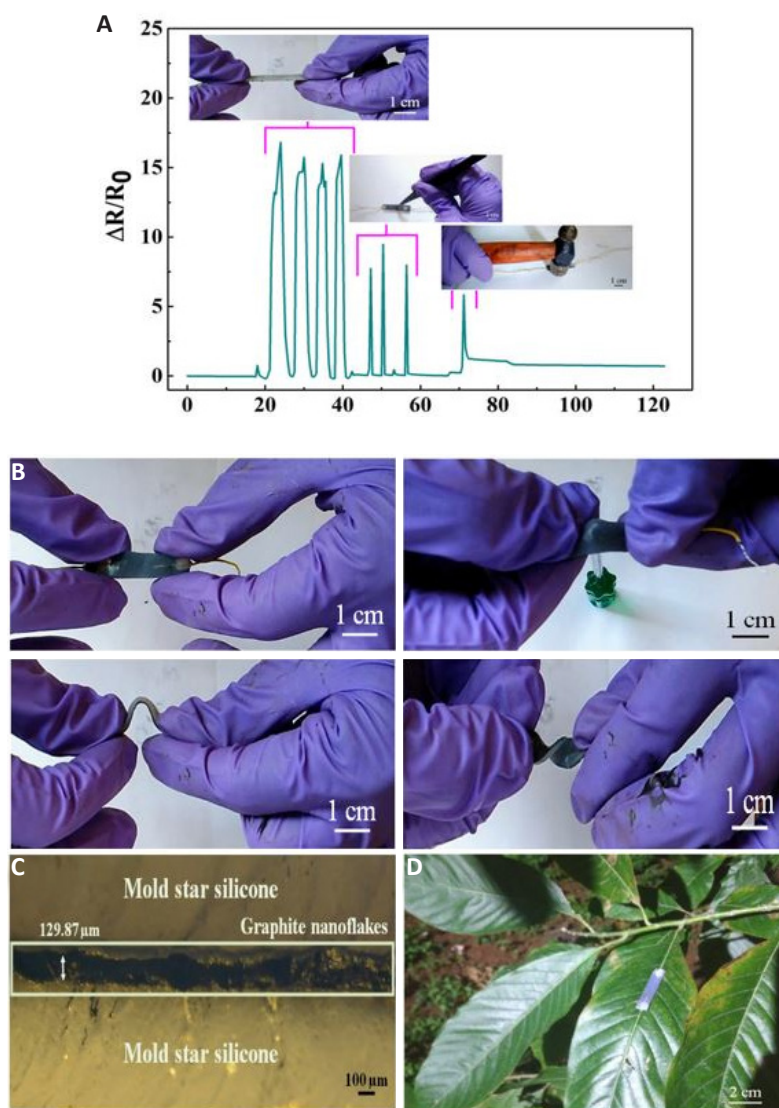


Figure 2. Illustration of the Mechanical Resilience of CSIs / Mold Star Nanocomposite Strain Sensors. (A) Mechanical resilience demonstration of strain sensor to puncturing deformations from a sharp object like a tweezer, and sudden impacts delivered from a hammer (the insets illustrate photographs captured during the experiments). (B) Puncturing, bending, and twisting of the strain sensor. (C) Cross-sectional image of the CSLs film on Mold star substrate (scale bar: 100μm). (D) Strain sensor placed on top of a leaf to demonstrate the light weight features of the nanocomposite.

stable electromechanical performance. For carrying out electromechanical studies, the carbonic film was electrically wired with two silver threads in order to obtain a wearable, skin-mountable, highly sensitive and stretchable strain sensor (Figure 2B).

Next, the evaluation of stretchability limit of carbonic films / Mold star nanocomposite-based strain sensors until electro-mechanical decomposition was carried out (Figure 3A). The electronic device was elongated at a stretching frequency of 0.1Hz until sensor insensitivity was observed. For this, the spray coated strain sensor was stretched for about 20 times until the sensor demonstrate a constant initial or base resistance before the evaluation of crucial strain sensor properties. It can be observed that the sample exhibit a steady and smooth electrical response until the strain levels were in the range of 0%-30%. Therefore, it can be concluded that the as-synthesized wearable strain

sensors could monitor and tolerate strain range of ~ 30%. Fascinatingly, the electrical conductivity of the strain sensors was fully restored when the external strains were reversed to 0%, indicating the elastic nature and self-crack-healing properties of the carbonic films / Mold star nanocomposite based stretchable strain sensors.

The strain sensitivity of carbonic films / Mold star nanocomposite-based strain sensors can be further increased by constructing carbonic films on a mold star silicone elastomer followed by the sensor pre-stretching procedures for 20 stretching-releasing cycles under a large-scale tensile strain of 50% as illustrated in Figure 3A. As depicted in Figure 3C, the strain sensitivity of carbonic films / Mold star strain sensors could be more than 2,185 through the pre-stretching of mold star silicone elastomers at 50% strain after the spray deposition process of carbon materials. The construction process of these strain sensing devices

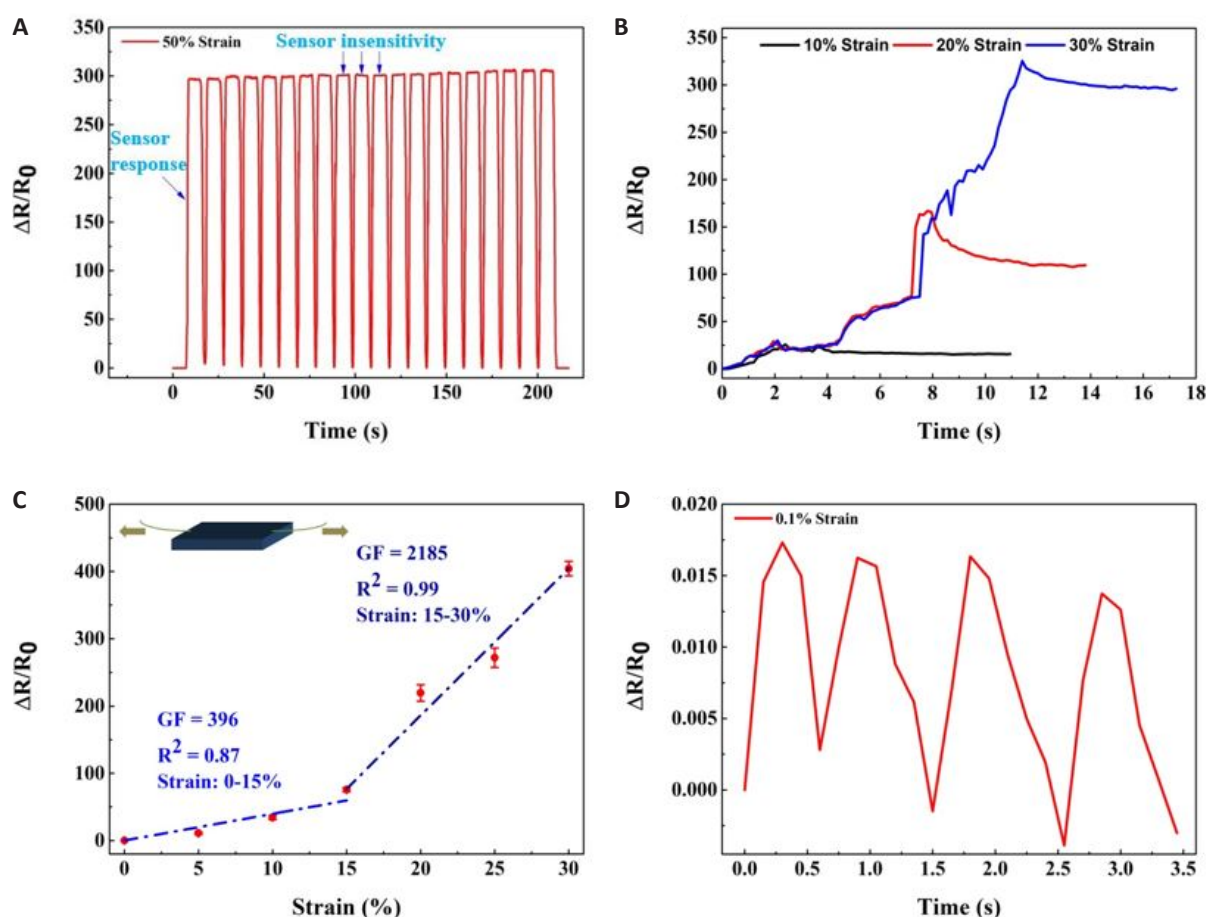


Figure 3. Electromechanical Properties, Performance and Characteristics of the CsIs / Mold Star Nanocomposite Strain Sensors. (A) The response of the strain sensor to tensile deformations during the pre-stretching process, that is, tensile strain levels more than that of the sensor response range (the electrical resistance variation of the strain sensor exhibits a stable tendency and sensor insensitivity at strain levels of 30%). (B) Relative resistance variation of the strain sensor in response to a tensile strain from 0% to 10%, 20%, and 30%. (C) Typical relative resistance variation versus strain within the sensing strain range, that is, 30% strain. Evaluation of the gauge factor, linearity, and sensing strain range. (D) The relative resistance variation of the strain sensor under a tiny strain of 0.1%. Evaluation of the low monitoring limit.

demonstrated high repeatability and such electronic sensors exhibited high sensitivity, reliability, stability, and durability. The electrical responses were highly reproducible. The recently reported state-of-the-art stretchable strain sensors delivered a much lower gauge factor values owing to the non-pre-stretching of the strain sensors before evaluating their electromechanical properties. For instance, Liu et al. reported a highly breathable anti-jamming copper-viscose yarn / Lycra textile strain sensor with a maximum gauge factor of 49.5^[8]. Wang et al. synthesized a high performance TPU / MWCNTs @MXene foam based stretchable strain sensor delivering a maximum gauge factor of 363^[46]. It is worth mentioning the numerous advantages of the pre-stretching process. The strain sensitivity of the sensor is tuned to its maximum value and the sensor signal is relatively stable, and reliable owing to the effective transfer of applied strains onto the sensor components. The high gauge factors of the strain sensors fabricated in this work is illustrated in Table 1.

As illustrated in Figure 3B, the electrical response of the strain sensor demonstrates slight overshoot behavior at the stretching-holding tensile strain levels of 10%, 20%, and

30% as a result of stress relaxation of mold star elastomers under external loads^[82]. The electrical responses exhibited a reliable and stable tendency after the sensor overshooting, indicating the reliable strain sensing performance of the spray coated strain sensors.

Figure 3C illustrates the strain-induced electrical resistance variations as the external strain was varied from 0% to 30%. The relative resistance variations were proportional to the external strain and exhibited a linearity with a coefficient of determination, $R^2 \sim 0.87$, and $R^2 \sim 0.99$ in the strain range of 0%-15%, and 15%-30%, respectively. The linearity and linear sensing range of the strain sensors fabricated in this work is illustrated in Table 2^[83-87].

The wearable strain sensor sensitivity is typically calculated through a GF measure, which is defined as

$$GF = \frac{\Delta R/R_0}{\epsilon}$$

Where $\Delta R/R_0 (= (R - R_0) / R_0)$ is the electrical resistance variation with mechanical strain, R_0 is the electrical resistance under a strain free state, that is, at 0% strain, and

Table 1. Summary of Sensing Performance Comparison in Terms of GFs and Sensing Strain Range for State-of-the-art Stretchable Strain Sensors

| Sensor Type | Fabrication Process | Materials | Gauge Factor (sensitivity) | Sensing Strain Range | Authors |
|-------------|---|--|----------------------------|----------------------|-------------------------------|
| Resistive | Salt-templating and dip-coating | MXene (Ti ₃ C ₂ T _x)- MWCNTs / TPU | 363 | 100% | Wang et al. ^[46] |
| Resistive | PAMD and lock-stitch embroidery | Copper nanoparticles-viscose yarn/Lycra fabrics | 49.5 | 200% | Liu et al. ^[8] |
| Resistive | Mechanical interlocking | Platinum (Pt)-Polyurethane acrylate (PUA) / PDMS | 11.5 | 5% | Pang et al. ^[75] |
| Resistive | Stencil printing | CNT / Poly(styrene- <i>b</i> -ethylene-butadiene) (SEBS) | 201.6 | 50% | Niu et al. ^[76] |
| Capacitive | Free-radical polymerization | Magnesium-Polylactic acid / Poly (glycerol sebacate)-Poly(octamethylene maleate (anhydride) citrate) | 3.3 | 15% | Boutry et al. ^[77] |
| Capacitive | Direct chemical reduction | Ag nanoparticles / PU-spandex fibres / PDMS-Ecoflex | 12 | 27.5% | Lee et al. ^[78] |
| Capacitive | Stencil printing | CNT / SEBS | 0.05 | 100% | Wang et al. ^[79] |
| Resistive | Low-pressure chemical vapour deposition | Gr / PDMS | 0.05 | 240% | Yong et al. ^[80] |
| Resistive | Spin coating | Gold (Au) / PDMS | 157 | 50 | Pan et al. ^[81] |
| Resistive | Spray deposition | CSLs / Mold star | 2185 | 30% | This Work |

Table 2. Summary of Sensing Performance Comparison in terms of Linearity and Linear Sensing Range for Previously Reported Stretchable Strain Sensors

| Sensor Type | Fabrication Process | Materials | Linear Sensing Range | Authors |
|-------------|--|---|---|----------------------------------|
| Resistive | Pulsed ultraviolet picosecond laser irradiation | Gr / Polyimide fabric | Linear up to 4% strain | Liu et al. ^[88] |
| Resistive | Vacuum filtration and chemical liquid etching | MXene (Ti ₃ C ₂ T _x) nanoparticle-nanosheet hybrid / PDMS | Linear up to 5% strain | Yang et al. ^[89] |
| Resistive | Coprecipitation, reduction, vacuum filtration, and casting | AgNWs-Gr hybrid / TPU | Linear up to 0.3% strain | Chen et al. ^[90] |
| Resistive | Atomic layer deposition | Pt nanoparticles (NPs) / Polyimide (kapton) | Linear in the sensing strain range of 1.12-7.2% | Aslanidis et al. ^[91] |
| Resistive | Sputter-coating | Au NPs / PDMS | Linear in the sensing strain range of 1.5-2% | Han et al. ^[92] |
| Resistive | CO ₂ laser irradiation | Gr / Filter paper | Linear up to 1% strain | Kulyk et al. ^[93] |
| Resistive | Spray deposition | CSLs / Mold star | High linearity (R ² >0.99 in the sensing strain range of 15-30%) | This Work |

$\varepsilon (= (L - L_0) / L_0)$ is the external tensile strain.

At small-scale strain range (0%-15%), a GF=396 was achieved, on the other hand, in the larger strain range (15%-30%), a GF_{max}=2,185 was achieved. Hence, the as-synthesized wearable strain sensing device based on carbonic films / Mold star nanocomposites outperformed the traditional metallic strain gauges (GF~2, ε <5%) in terms of both large strain sensitivity (or GF) and stretchability (or strain range)^[1,83]. Even though previously reported carbon nanomaterials-based strain sensors demonstrated a high stretchability (~300% strain), the strain sensitivities were normally restricted to very minute levels and exhibited a gauge factor (GF_{max}~13.1) confining their applicability for entire-range human motion monitoring where multi-scale strain sensing ability (both small-scale and large-scale

human motion monitoring) is typically required^[84]. This work reports carbon nanomaterials-based strain sensors with both high sensitivity and high stretchability simultaneously for the full-range practical sensing applications.

The evaluation of strain detection limit of carbonic films / Mold star nanocomposite was carried out next. Figure 3D depicts the relative resistance variation versus time data under minute strain scales. It can be observed that the dynamic strain variation could be effectively monitored even under a minute cyclic strain of 0-0.1%. Moreover, a stretching strain with a small-scale displacement of around 0.02mm was subjected onto the electronic device, corresponding to a minute strain level of 0.1%. As presented in Figure 3D, such a minute strain could be well monitored with a relative resistance variation of about ~ 1.5%. The low monitoring

Table 3. Summary of Sensing Performance Comparison in Terms of Low Monitoring Limit for Previously Reported Stretchable Strain Sensors

| Sensor Type | Fabrication Process | Materials | Low Monitoring Limit (Strain %) | Authors |
|-------------|------------------------------------|--|---------------------------------|--------------------------------|
| Resistive | Wet-spinning and dip-coating | AgNWs-CNTs / hermoplastic PU | 0.5 | Liu et al. ^[94] |
| Resistive | Stirring coating | Graphene nanoplatelets-carbon black (CB)-cotton cloth / Ecoflex | 0.5 | Souri et al. ^[21] |
| Resistive | Drop-casting and vacuum filtration | CNTs / PDMS | 0.5 | Nankali et al. ^[95] |
| Resistive | Salt-templating and dip-coating | MXene (Ti ₃ C ₂ T _x)- MWCNTs / TPU | 5 | Wang et al. ^[46] |
| Resistive | Latex film-forming | CNTs / Carboxylic styrene butadiene rubber | 1 | Lin et al. ^[74] |
| Resistive | Spray deposition | CSLs / Mold star | 0.1 | This Work |

limit of the strain sensors fabricated in this work is illustrated in Table 3.

The carbonic films demonstrated excellent mechanical stability with strain range up to 30% without any noticeable detachment from Mold star silicone elastomer (Figure 4A and 4E). Figure 4A illustrates the electrical-mechanical characteristics from the proposed electronic device. The performance of the spray coated strain sensors were examined over five dynamic cyclic strains for both small-scale (~ 5% strain) and large-scale (~ 30% strain) strain loading states at a fixed tensile frequency of 0.05Hz. A highly reversible electrical response with minimal drift and noise can be clearly noticed during the dynamic cyclic deformations. In addition, it can be noticed from Figure 4A that the spray coated carbonic films / Mold star strain sensor exhibit a stable electrical response to a tiny mechanical deformation as small as $\epsilon \sim 5\%$ which demonstrates that the electronic device will be beneficial for the monitoring of human physiology and tiny deformations. This electronic device demonstrated a prominent electrical conductivity recovery, much better than their corresponding wet-spun PU / poly(3,4-ethylenedioxythiophene): poly(styrenesulfonate) (PEDOT:PSS) composite strain sensor^[85]. The electrical resistance of carbonic films / Mold star strain sensors increase in a smooth and progressive manner with increased levels of external strains and recovers smoothly to their original values as the external strain was reversed back to the strain free state, that is, 0%. The strain responsiveness was fully reversible under a large-scale dynamic strain of 0%-30%-0% with negligible hysteretic performance. In contrast, the wet-spun PU / PEDOT:PSS composite lost its initial conductivity and became more insulative when the external strain level increased to 50%, and remained at this state even after the removal of the external strain when reversed back to 0%^[85]. This type of hysteretic performance was attributed to the loss of fibrillar and lamellar orientation, the irreversible deformations while stretching, and the slipping of polymeric chains in hard segment domains.

After that, the reliability of the as-synthesized strain

sensor was evaluated by examining the amplitude at a stretching frequency range of 0.04-0.15Hz (Figure 4B). A noise-free electrical response exhibiting negligible drift in the sensor response can be clearly noticed which implies that the carbonic films / Mold star nanocomposite-based strain sensors demonstrate almost negligible dependency upon external stretching frequency amplitudes. These results imply that the spray coated strain sensors demonstrate reliable and durable frequency independent electromechanical characteristics under mechanical strains. It is worth to mention that the above-mentioned sensor evaluation tests demonstrate the prominent properties of the carbonic films / Mold star nanocomposite-based strain sensor with regard to ultra-high sensitivity, a large dynamic sensing range or high stretchability, fast response rate, excellent reversibility with negligible hysteresis properties, and excellent durability and stability, which are believed to be the crucial requirements in practical wearable applications, for example, in multi-scale human motion monitoring.

The electromechanical characteristics of the spray coated strain sensors during the stretching and holding was also examined (Figure 4C). The sensor response was evaluated by applying tensile strains of 10%, 20%, and 30% onto the device, and holding it for a fixed time, followed by releasing from the stretched state. It can be noticed that slight overshooting is produced in the electrical response owing to the stress relaxation of mold star elastomers. The sensor response is reliable and stable at the specific tensile strain level or mechanical deformation and increases with increment in the amplitude of tensile strains. The distinguishing sensor response demonstrates the attractive strain monitoring features of the spray coated strain sensors.

The carbonic films / Mold star nanocomposite-based strain sensors also demonstrated a prominent durability. Figure 4D illustrates the examination of sensor performance under a large-scale dynamic stretch-release strain of 0-30% at a stretching frequency of 0.04Hz. As shown in the figure, the as-synthesized wearable strain sensor exhibits stable

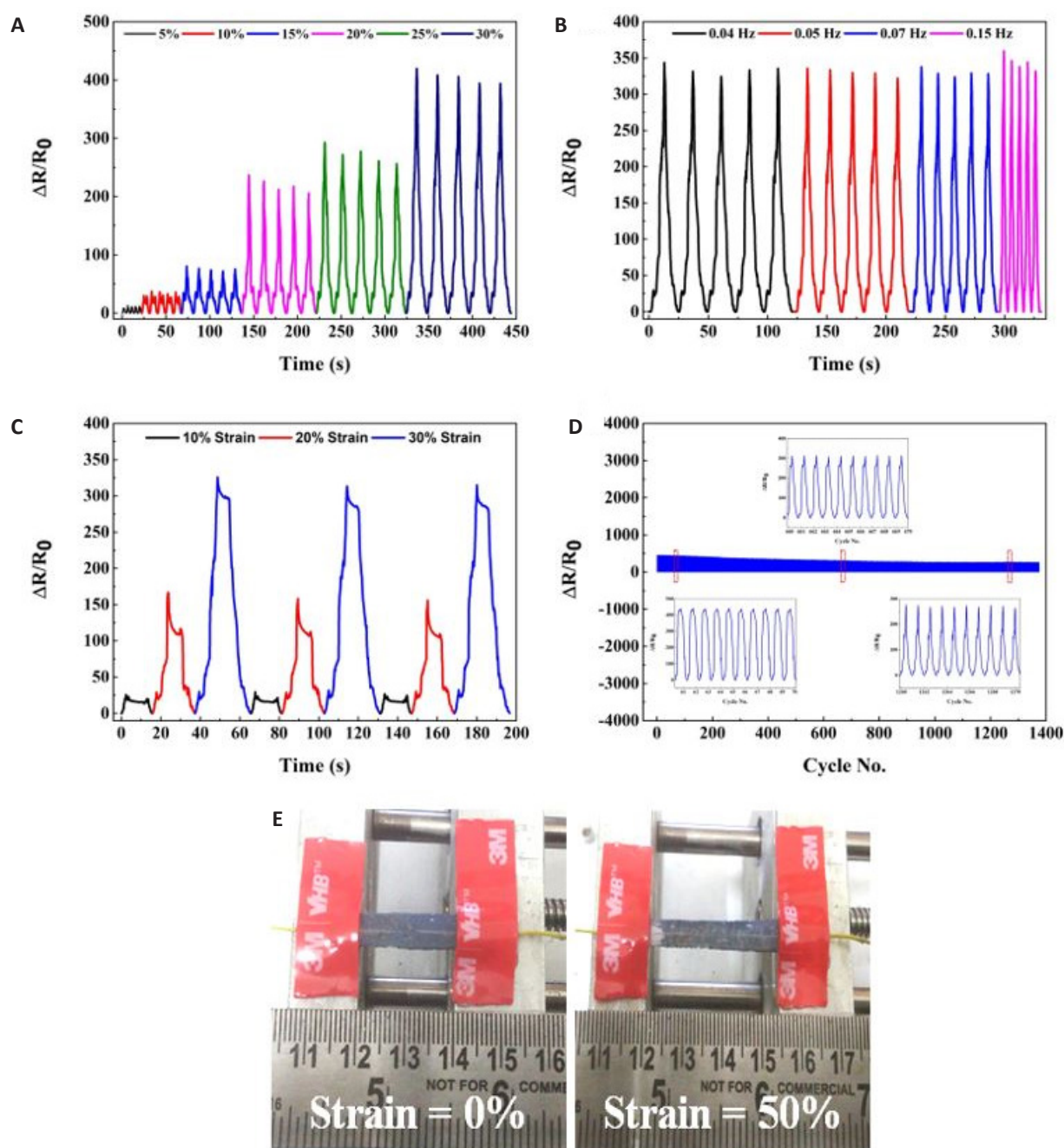


Figure 4. Strain Sensing Performance Characterization of the CsIs / Mold Star Nanocomposite Strain Sensors. Strain sensor response for multi-scale loading, unloading deformations and dynamic loadings. (A) Dynamic cyclic studies of relative resistance variation of the sensor upon loading to various strains. (B) Frequency response of the sensor from 0.04 Hz to 0.15 Hz. (C) Relative resistance variation of the sensor at various static strain loading instances. (D) Cyclic stability studies of the sensor in more than 1,300 loading cycles at the full sensing strain range of 30%. The mechanical deformations were from 0% strain and large-scale strain of 30%, respectively. (E) Photographs of the sensor at strain loading instances.

and reproducible electrical responses for more than 1,300 dynamic cycles under a large-scale tensile strain of 30%. The wearable device demonstrated a stable, reliable, and predictable relative resistance variation during the long-term stretching-releasing process. The relative resistance changes of the strain sensor demonstrated only a slight variation after the dynamic investigation, indicating the prominent durability of the carbonic films / Mold star nanocomposite based stretchable sensors. The dynamic durability of the strain sensors fabricated in this work is illustrated in Table 4.

Figure 4E illustrates the large-scale stretching ability of the spray coated sandwich structural stretchable strain sensors. At the present moment, stretchable and wearable strain sensors are being manufactured enormously through the deposition or embedding of active sensor materials (or functional materials) onto the stretchable supporting materials (or stretchable substrates)^[86]. Chen et al. fabricated fabric-based strain sensors with the sensitivities of 2.15 ± 0.28 ^[87]. In many stretchable strain sensors, the surface morphology and the respective strain sensing performance

Table 4. Summary of Sensing Performance Comparison in Terms of Durability and Stability for Previously Reported Stretchable Strain Sensors

| Sensor Type | Fabrication Process | Materials | Dynamic Durability (stretching-releasing cycles) | Authors |
|-------------|---------------------------------|---|---|------------------------------|
| Resistive | Spray coating | AgNWs-acrylate / PDMS | 500 | Kong et al. ^[96] |
| Resistive | Inkjet printing | AgNWs-acrylate / PDMS | 100 | Huang et al. ^[97] |
| Resistive | Dip coating | RGO/nylon/PU | 120 | Cai et al. ^[98] |
| Resistive | Salt-templating and dip-coating | MXene (Ti ₃ C ₂ T _x)-MWCNTs / TPU | 200 | Wang et al. ^[46] |
| Resistive | Solvent casting | Poly(2- acrylamido-2-methyl-1-propanesulfonic acid)-polyaniline-phytic acid (PA) / 3M VHB-4910 tape | 70 | Lu et al. ^[99] |
| Resistive | Rod coating and peeling | AgNWs / TPU | 200 | Wang et al. ^[100] |
| Resistive | Spray deposition | CSLs / Mold star | More than 1,300 | This Work |

can become unreliable without any problem even through the application of a tiny strain (or deformation) like a human finger touch.

3.2 Working and Sensing Mechanisms

In order to investigate the phenomena of ultra-large strain sensitivity of the Carbonic sensing layers / Mold star nanocomposite-based strain sensors exhibited due to the applied strains, the changes in the structural characteristics of the conductive thin films were examined at various stretching strain levels of up to 90% with a step increment of 30% strain (Figure 5A). Through the simultaneous consideration of Figure 3D, at a minute strain level of 0.1%, the carbon conductive thin film is still intact without any noticeable destruction in its microstructure. Therefore, the strain sensitive response is primarily controlled by the geometrical effects and the contacted electric resistance of the graphitic materials.

$$R = \rho \frac{L}{A}$$

where L is the sensor length, A is the cross-sectional area of functional sensor materials, and ρ is the electrical resistivity of the strain sensor.

At a moderate strain level of 15% (Figure 3C), slight destruction / damage of the conductive thin film can be noticed with the generation of structural cracks with jagged edges which connect with each other in a horizontal plane to the Mold star silicone elastomeric substrate and leading to a rapid electrical resistance change to the applied external strains. Owing to the dual-layer system, that is, Carbonic sensing layers / Mold star, with considerable Young's modulus mismatch, the jagged crack edges are partly overlapped and, in this occasion, the crossing of the electrons occur through the overlapped electrically conductive fragments.

With further stretching (strain levels more than 15%), significant destruction / damage of the conductive thin film occur and the crack edges lose their overlapped area as well

as the electrical connectivity leading to the enhancement of electrical resistance exhibiting consistency with the data presented in Figure 3C, and previous works^[48]. This feature is schematically illustrated in Figure 5B. Moreover, in this occasion, the separation of the crack edges exhibit quantum tunneling junctions with distance in the range of tunneling cut-off and the electron transport takes place due to the tunneling phenomena.

$$R = \frac{V}{AJ} = \frac{h^2 d}{Ae^2 \sqrt{2m\lambda}} \cdot \exp\left(-\frac{4\pi d}{h} \sqrt{2m\lambda}\right)$$

where V is the electrical potential difference, J denotes the current density due to tunneling, A is the tunneling junction's cross-sectional area, d is the distance value between electrically conductive nanomaterials, h is Planck's constant, e is the single-electron charge, m is the electron mass, and λ is the energy barrier height.

In this situation, the Carbonic sensing layers / Mold star nanocomposite-based strain sensors demonstrate ultra-large variation in electrical resistance leading to ultrahigh gauge factors. Therefore, these ultrasensitive wearable strain sensors can be employed in practical application for monitoring versatile-range human motions including vocal cord vibrations, artery pulse waveforms, face expressions, and human articular joint motions.

At the initial state of 0% strain, the conductive film surface is clear and smooth, and the nanomaterial networks are integrated. At a stretching condition, the conductive film starts to gradually break and rupture. The nanomaterials slide / disconnect from each other in the mold star matrix and the loss of overlapping area occurs. Structural cracks are observed in the conductive film resulting in the resistance variation with a high sensitivity and strain sensing range.

3.3 Recognition of Human Epidermal Movements

Apart from monitoring of stretching strains, the carbonic films / Mold star nanocomposites can also be utilized as bending deformation / strain monitors. As illustrated in

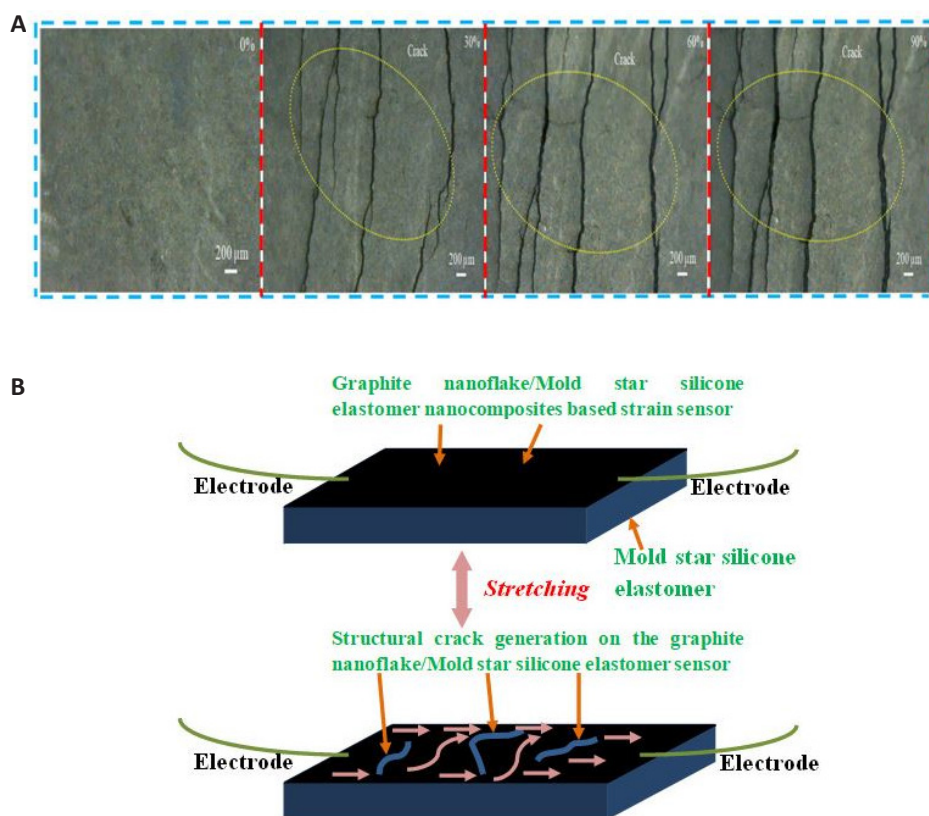


Figure 5. Working Mechanisms of CSLs / Mold Star Nanocomposite Strain Sensors. (A) Optical images illustrating the surface morphology of CSLs film at different strain loading conditions of 0%, 30%, 60%, and 90%, respectively. Scale bar: 200 μ m. (B) Schematic of the working mechanisms or strain sensing mechanisms. The schematic illustrates the electrical conduction mechanisms of the CSLs / Mold star nanocomposite strain sensors corresponding to the morphological evolution.

Figure 6, and Figure 7, the evaluation of sensing abilities to tensile bending and compressive bending at different dynamic strains during human motion monitoring were carried out. The electrical responses were stable, reliable, predictable, and exhibited prominent electrical response recovery features, implying minimal hysteresis and permanent set. For tensile bending, the electrical resistance increased with higher bending strains owing to the stretched carbonic conductive network. In contrast, for compressive bending, the electrical resistance decreased with increased bending strains owing to the overlapping and wrinkling of the carbonic conductive network, leading to improved conductive pathways. These results demonstrate the superior design and fabrication strategy of the as-synthesized carbonic films / Mold star nanocomposite-based strain sensors.

The Carbonic sensing layers / Mold star silicone elastomer strain sensor could be laminated onto the different locations of the human body with the assistance of Skin-Tite bioadhesive for monitoring diverse-range human movements from minute scale (cheek deformation, eye blinking, frowning, and laryngeal prominence movement) to large-scale (finger bending, wrist, elbow, and knee joint bending). The skin-lamination methods of the existing strain sensors are illustrated in Table 5. Figure 7 shows the relative resistance variation for cyclic bending

/ recovering of human finger, wrist, elbow, and knee at a frequency of 0.15, 0.06, 0.12, and 0.10Hz, respectively. The electrical resistance variation demonstrates fast responsiveness with favourable reproducibility and this response could be attributed to the structural variations in Carbonic sensing layers conductive networks due to applied strains. Upon recovering from the bending state, the electrical resistance recovers its original value fully in a rapid manner. The wearable strain sensors demonstrated a stable responsiveness to various mechanical deformations with favourable reproducibility during the cyclic bending / recovering of various articular joints. The noise levels during these experiments were minimized by achieving an intimate and conformal lamination of the device with the human epidermal surface using Skin-Tite bioadhesive.

Moreover, using the data captured during the bending and holding process of a finger (Figure 7A), the response and recovery time of Carbonic sensing layers / Mold star silicone elastomer composite strain sensors were evaluated reliably. In order to evaluate the response time of the carbonic films / Mold star nanocomposite-based strain sensors, large-scale dynamic strains were applied onto the devices instantaneously at a large stretching frequency of 0.15Hz. The response / recovery time of wearable strain sensors are estimated as the time required to reach the steady state. Using this, the response and recovery time of

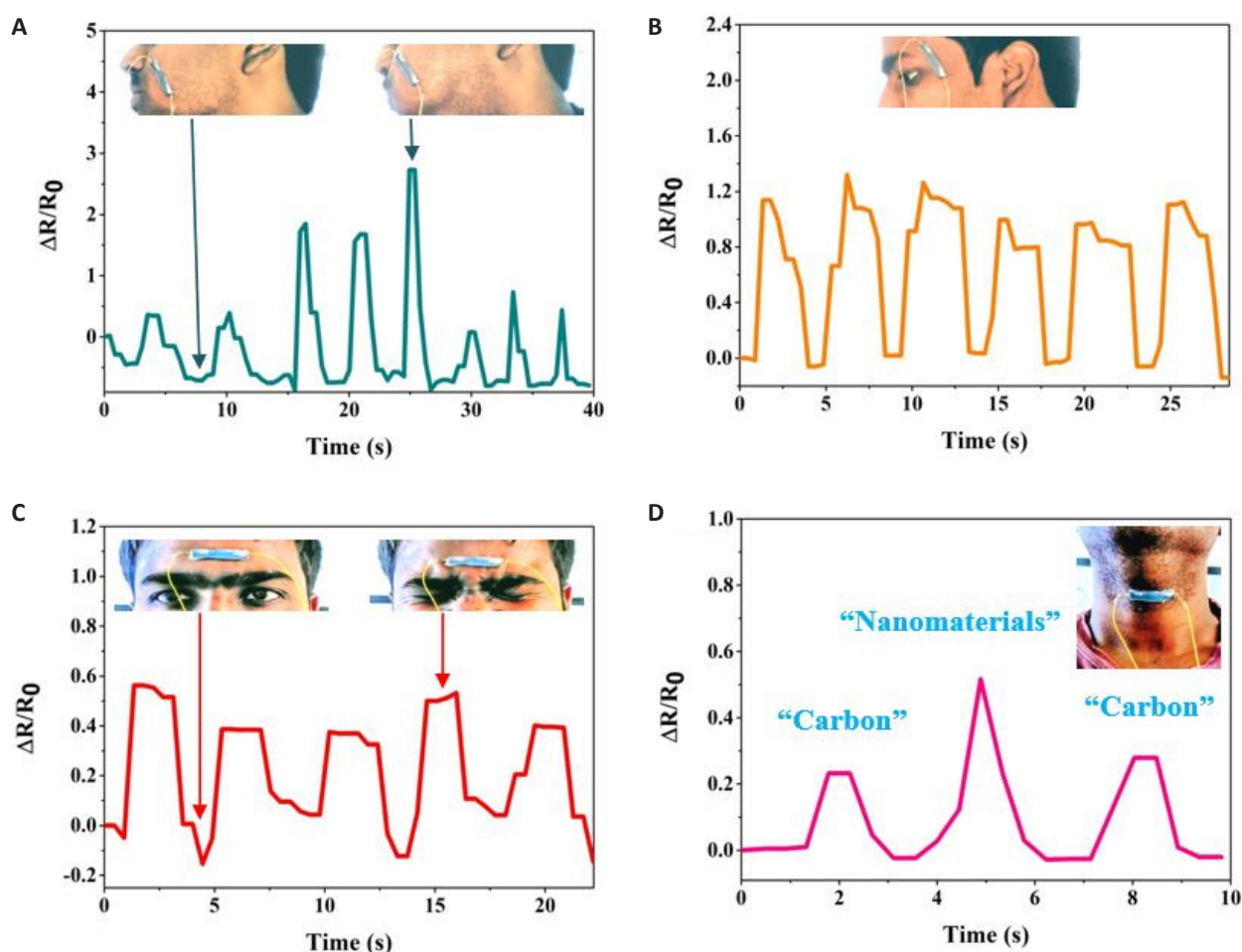


Figure 6. Using the Sensor for Epidermal Movement Monitoring. Real-time detection of small-scale human muscle motions with the CSLs / Mold star nanocomposite strain sensor. Sensor response to the tiny muscle movements induced by the (A) cheek relaxation/expansion, (B) eye canthus motions, (C) and forehead frowning action. (D) Real-time electrical response of the sensor during the larynx motions (or vocal cord vibrations) induced by the phonation of various words namely, “Carbon”, and “Nanomaterials”.

the as-fabricated wearable strain sensors were estimated to be lesser than 500ms, respectively, from the dynamic relative resistance variation versus time data within one bending / holding / recovering cycle, implying its fast and swift strain responsiveness and recovery. Through the consideration of measurement delays, the real response time of the spray coated strain sensors presented here is believed to be significantly faster. The as-fabricated strain sensors demonstrate quicker response rate than the recently reported state-of-the-art stretchable strain sensors. Wu et al. reported a PDMS / Gr (vertical nanosheets) / PDMS nanocomposite-based stretchable strain sensors exhibiting a response rate of 960ms^[82].

Owing to the ultra-large strain sensitivity of Carbonic sensing layers / Mold star silicone elastomer composite strain sensors, the devices can also be employed for monitoring face expressions and larynx motions including cheek expansion, eye blinking, frowning, and speech recognition (Figure 6). The wearable strain sensor demonstrates its fascinating capability of detecting minute-scale mechanical deformations in a rapid, stable, and reproducible manner. Moreover, large-scale deformations

from various joint bending movements demonstrated a significantly larger relative resistance variation than the minute-scale muscle motions exhibited by various facial expressions, indicating the ability of the Carbonic sensing layers / Mold star silicone elastomer composite based wearable strain sensor to differentiate the human bodily motions with discrete strain scales, and therefore can be employed for multi-scale sensing. These sensing demonstrations using the Carbonic sensing layers / Mold star silicone elastomer composites indicate the potential applicability of these electronic devices in the next-generation electronics including artificial skin, soft robotics, and human-machine interactive systems.

In this work, the wearable strain sensors demonstrated negligible noise in the electrical responses during the monitoring of mechanical deformations. The external environmental and atmospheric factors such as temperature, pressure, water, oil, and sweat had minimal effect on the sensor response owing to the sandwich structural design of the sensor wherein the sensing film was fully encapsulated within the ultra-soft mold star elastomers. The external factors vary the sensor response in an unreliable manner

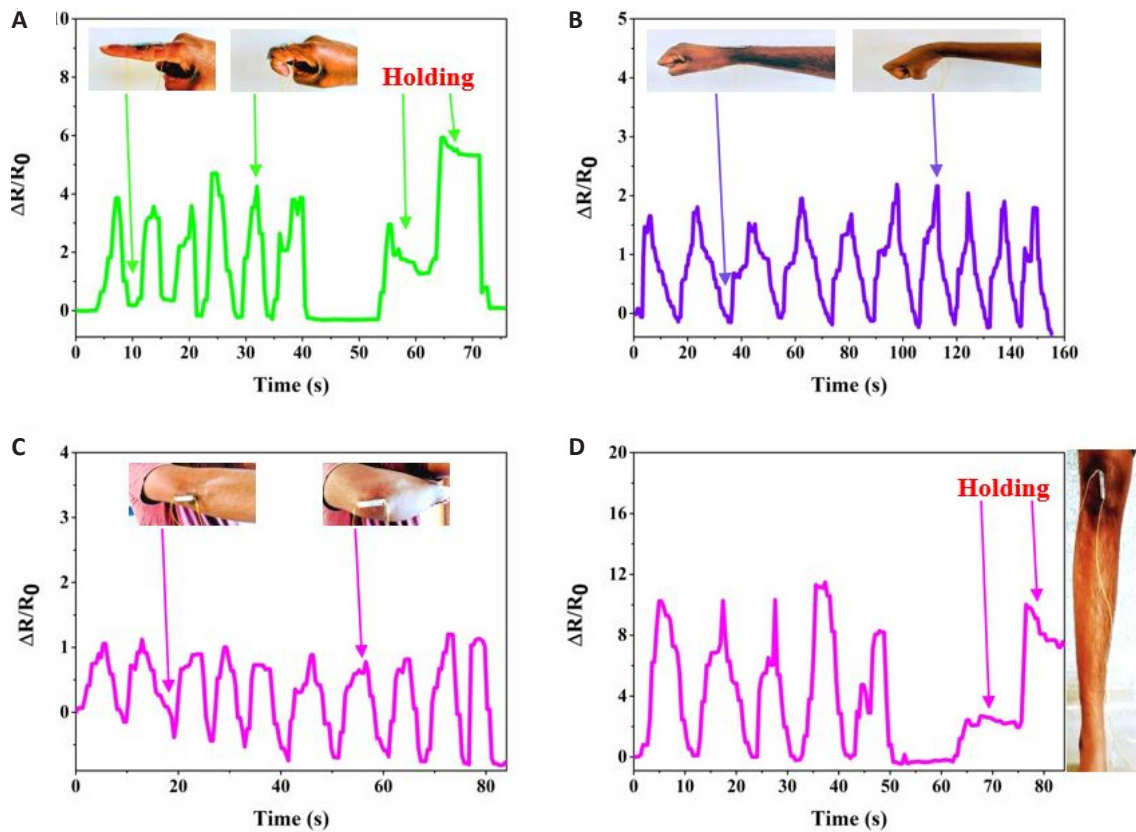


Figure 7. Using the Sensor for Epidermal Movement Monitoring. Real-time monitoring of large-scale human motions with the CSLs / Mold star nanocomposite strain sensor. Sensor response to the energetic muscle movements induced by the (A) finger bending, (B) wrist bending, (C) elbow bending, (D) and knee bending motions.

Table 5. Summary of the Lamination Procedures and Corresponding Maximum Relative Resistance Variation During Application

| Sensor Type | Fabrication Process | Materials | Epidermis Lamination Method | Maximum Relative Resistance Variation ($\Delta R/R_0$) | Authors |
|-------------|---|--|--|--|---------------------------------|
| Resistive | Solution mixing-casting | CNTs-CB / PDMS | PU film | 2.2 | Zheng et al. ^[101] |
| Resistive | Lockstitch process using sewing machine | Silver (Ag)-Nylon-Lycra / Textile fabric | Sensor stitching on woven fabric | 7 | Park et al. ^[102] |
| Resistive | Drop-casting and spin-coating | CuNWs-PEDOT:PSS / Ecoflex | Tegaderm film | 4.5 | Han et al. ^[18] |
| Resistive | Aerosol jet printing and spin-coating | AgNWs / Ecoflex | Self-attachment via van der Waals interactions | 0.0065 (ΔR) | Herbert et al. ^[103] |
| Resistive | One-step photolithography, ultrasonication and spin-coating | AgNWs-acrylate / PDMS | Self-attachment | 8.75 | Liu et al. ^[48] |
| Resistive | Sputtering | Pt / PUA | Commercial tape | 7 (ΔR) | Kang et al. ^[73] |
| Resistive | Spray deposition | CSLs / Mold star | Skin-Tite bioadhesive | 12 | This Work |

leading to inaccurate and non-precise measurements during the wearable occasions. These factors are specifically critical for simple structured strain sensors wherein the sensing film is embedded in the flexible / stretchable matrix without any encapsulating agent.

Finally, the sensing performance and human motion monitoring methods for state-of-the-art stretchable strain sensors have been thoroughly compared with the spray coated strain sensor in Tables 1-5. The current results indicate that the recently fabricated CSLs / Mold star silicone elastomer nanocomposite based stretchable strain

sensors have realized a fascinating co-occurrence of ultra-high strain sensitivity ($GF=2185$ in the sensing strain range of 15-30%) with an extensive dynamic range of 30% strain, prominent linearity ($R^2>0.99$ in the sensing strain range of 15-30%), low monitoring limit, high stability and durability for large-scale tensile deformations. Specifically, Table 1 illustrates the previously reported state-of-the-art stretchable strain sensors fabricated via different procedures for critical strain sensor property comparison, GFs, and sensing strain range. It can be noticed that the spray coated CSLs / Mold star silicone elastomer nanocomposite based stretchable strain sensors demonstrate ultrasensitive sensing

performance and outperform the previously reported state-of-the-art stretchable strain sensors, specifically in terms of gauge factors. Almost all the strain sensors exhibit low sensitivities. In contrast, the spray coated stretchable strain sensors are ultrasensitive, and highly stretchable. Thus, it is envisioned that these recently fabricated strain sensors will be fascinating for future wearable electronics for a diverse-range of crucial practical applications.

4 CONCLUSION

In summary, this work reported the stretchable strain sensors with ultra - high strain sensitivity and a wide sensing strain range simultaneously designed utilizing CSLs / Mold star silicone elastomer nanocomposites. The strain sensitivity of the stretchable strain sensors is prominently enhanced by more than 1,000 times relative to that of traditional metallic foil - based strain gauge sensors. The outstanding strain sensitivity was an outcome of mechanical cracks production in the electrically conductive film while strain concentration during tensile deformations. The as - fabricated stretchable strain sensors demonstrated an ultrasensitive gauge factor of 2,185 and a sensing strain range of 30%. In addition, ultra-low monitoring limit (less than 0.1% strain), low overshoot behavior, and high durability (more than 1,300 stretch-release cycles under a large-scale strain of 30%) are prominent features of the stretchable strain sensors. Through sensing demonstrations of practical human motion monitoring applications, the stretchable strain sensors can be envisioned as critical components for future wearable electronics with smart functionalities, including but not confined to human motion / health monitoring, electronic skins, soft robotics, augmented reality and virtual reality, human-machine / computer interfaces, and sports performance monitoring. It is believed that the methodologies presented in this research set forth a novel and low - cost stretchable strain sensor with a scalable approach to obtain prominent sensing performance, and may facilitate the sensitivity enhancement of numerous flexible, and stretchable devices.

Conflicts of Interest

There are no conflict of interest to declare.

Author Contribution

Independent research and full-contribution by Madhavan R (Independent Scientist).

Funding Statement

The research was self-funded by the author, Madhavan R (Independent Scientist).

Abbreviation List

AgNWs, Silver nanowires
CB, Carbon black
CNT, Carbon nanotube
CSLs, Carbonic sensing layers

CuNWs, Copper nanowires
GF, Gauge factor
Gr, Graphene
MWCNTs, Multiwalled carbon nanotubes
NPs, Nanoparticles
PA, Phytic acid
PAMD, Polymer-assisted metal deposition
PDMS, Polydimethylsiloxane
PEDOT:PSS, Poly(3,4-ethylenedioxythiophene):poly(styrene sulfonate)
PET, Polyethylene terephthalate
PU, Polyurethane
PUA, Polyurethane acrylate
SEBS, Poly(styrene-*b*-ethylene-butadiene)
TPU, Thermoplastic polyurethane
VHB, Very High Bond

References

- [1] Madhavan R. Nanocrack-based ultrasensitive wearable and skin-mountable strain sensors for human motion detection. *Mater Adv*, 2022; 3: 8665-8676.[DOI]
- [2] Madhavan R. Network crack-based high performance stretchable strain sensors for human activity and healthcare monitoring. *New J Chem*, 2022; 46: 17596-17609.[DOI]
- [3] Jeong Y, Kim J, Xie Z et al. A skin-attachable, stretchable integrated system based on liquid GaInSn for wireless human motion monitoring with multi-site sensing capabilities. *Npg Asia Mater*, 2017; e443.[DOI]
- [4] Huang CB, Witomska S, Aliprandi A et al. Molecule-Graphene Hybrid Materials with Tunable Mechanoreponse: Highly Sensitive Pressure Sensors for Health Monitoring. *Adv Mater*, 2019; 31: 1804600.[DOI]
- [5] Xu X, Chen Y, He P et al. Wearable CNT/Ti₃C₂T_x MXene/PDMS composite strain sensor with enhanced stability for real-time human healthcare monitoring. *Nano Res*, (2021).[DOI]
- [6] Fang X, Tan J, Gao Y et al. High-performance wearable strain sensors based on fragmented carbonized melamine sponges for human motion detection. *Nanoscale*, 2017; 9: 17948-17956.[DOI]
- [7] Xiong J, Chen J, Lee P. Functional Fibers and Fabrics for Soft Robotics, Wearables, and Human-Robot Interface. *Adv Mater*, 2021; 33: 2002640.[DOI]
- [8] Liu Z, Zheng Y, Jin L et al. Highly Breathable and Stretchable Strain Sensors with Insensitive Response to Pressure and Bending. *Adv Funct Mater*, 2021; 31: 2007622.[DOI]
- [9] Yang T, Jiang X, Zhong Y et al. A Wearable and Highly Sensitive Graphene Strain Sensor for Precise Home-Based Pulse Wave Monitoring. *ACS Sensors*, 2017; 2: 967-974.[DOI]
- [10] Song Z, Li W, Han F et al. Breathable and Skin-Mountable Strain Sensor with Tunable Stretchability, Sensitivity, and Linearity via Surface Strain Delocalization for Versatile Skin Activities Recognition. *Acs Appl Mater Inter*, 2018; 10: 42826-42836.[DOI]
- [11] Park J, Hyun W, Mun S et al. Highly Stretchable and Wearable Graphene Strain Sensors with Controllable Sensitivity for Human Motion Monitoring. *Acs Appl Mater Inter*, 2015; 7:

- 6317-6324.[\[DOI\]](#)
- [12] Wang S, Cheng H, Yao B et al. Self-Adhesive, Stretchable, Biocompatible, and Conductive Nonvolatile Eutectogels as Wearable Conformal Strain and Pressure Sensors and Biopotential Electrodes for Precise Health Monitoring. *Acs Appl Mater Inter*, 2021; 13: 20735-20745.[\[DOI\]](#)
- [13] Liu Z, Qi D, Hu G et al. Surface Strain Redistribution on Structured Microfibers to Enhance Sensitivity of Fiber-Shaped Stretchable Strain Sensors. *Adv Mater*, 2018; 30: 1704229.[\[DOI\]](#)
- [14] Amjadi M, Pichitpajongkit A, Lee S et al. Highly Stretchable and Sensitive Strain Sensor Based on Silver Nanowire-Elastomer Nanocomposite. *Acs Nano*, 2014; 8: 5154-5163.[\[DOI\]](#)
- [15] Roh E, Kim D, Hwang BU et al. Stretchable, Transparent, Ultrasensitive, and Patchable Strain Sensor for Human-Machine Interfaces Comprising a Nanohybrid of Carbon Nanotubes and Conductive Elastomers. *ACS Nano*, 2015; 9: 6252-6261.[\[DOI\]](#)
- [16] Yin J, Hinchet R, Shea H et al. Wearable Soft Technologies for Haptic Sensing and Feedback. *Adv Funct Mater*, 2021; 31: 2007428.[\[DOI\]](#)
- [17] Wang K, Yap LW, Gong S et al. Nanowire-Based Soft Wearable Human-Machine Interfaces for Future Virtual and Augmented Reality Applications. *Adv Funct Mater*, 2021; 31: 2008347.[\[DOI\]](#)
- [18] Han S, Liu C, Xu H et al. Multiscale nanowire-microfluidic hybrid strain sensors with high sensitivity and stretchability. *Npj Flex Electron*, 2018; 16.[\[DOI\]](#)
- [19] Yang YF, Tao LQ, Pang Y et al. An Ultrasensitive Strain Sensor with a Wide Strain Range Based on Graphene Armour Scales. *Nanoscale*, 2018; 10: 11524-11530.[\[DOI\]](#)
- [20] Kurian AS, Souri H, Mohan V et al. Highly Stretchable Strain Sensors Based on Polypyrrole-Silicone Rubber Composites for Human Motion Detection. *Sens Actuators*, 2020; 312: 112131.[\[DOI\]](#)
- [21] Souri H, Bhattacharyya D. Bhattacharyya Highly sensitive, stretchable and wearable strain sensors using fragmented conductive cotton fabric. *J Mater Chem C*, 2018; 6: 10524-10531.[\[DOI\]](#)
- [22] Sun Z, Yang S, Zhao P et al. Skin-like Ultrasensitive Strain Sensor for Full-Range Detection of Human Health Monitoring. *Acs Appl Mater Inter*, 2020; 12: 13287-13295.[\[DOI\]](#)
- [23] Wang S, Xiao P, Liang Y et al. Network Cracks-based Wearable Strain Sensors for Subtle and Large Strain Detection of Human Motions. *J Mater Chem C*, 2018; 6: 5140-5147.[\[DOI\]](#)
- [24] Li Y, He T, Shi L et al. Strain Sensor with Both a Wide Sensing Range and High Sensitivity Based on Braided Graphene Belts. *Acs Appl Mater Inter*, 2020; 12: 17691-17698.[\[DOI\]](#)
- [25] Yan C, Wang J, Kang W et al. Highly Stretchable Piezoresistive Graphene-Nanocellulose Nanopaper for Strain Sensors. *Adv Mater*, 2014; 26: 2022-2027.[\[DOI\]](#)
- [26] Duan L, R. D'Hooge D, Cardon L. Recent progress on flexible and stretchable piezoresistive strain sensors: From design to application. *Prog Mater Sci*, 2020; 114: 100617.[\[DOI\]](#)
- [27] Ramli NA, Nordin AN, Azlan NZ. Development of low cost screen-printed piezoresistive strain sensor for facial expressions recognition systems. *Microelectron Eng*, 2020; 234: 111440.[\[DOI\]](#)
- [28] Deng C, Lan L, He P et al. High-Performance Capacitive Strain Sensors with Highly Stretchable Vertical Graphene Electrodes. *J Mater Chem C*, 2020; 8: 5541-5546.[\[DOI\]](#)
- [29] You B, Kim Y, Ju BK et al. A wearable piezocapacitive pressure sensor with a single layer of silver nanowire-based elastomeric composite electrodes. *J Mater Chem A*, 2016; 4: 10435-10443.[\[DOI\]](#)
- [30] Nur R, Matsuhisa N, Jiang Z et al. A Highly Sensitive Capacitive-type Strain Sensor Using Wrinkled Ultrathin Gold Films. *Nano Lett*, 2018; 18: 5610-5617.[\[DOI\]](#)
- [31] Feng P, Yuan Y, Zhong M et al. Integrated Resistive-Capacitive Strain Sensors Based on Polymer-Nanoparticle Composites. *Acs Appl Nano Mater*, 2020; 3: 4357-4366.[\[DOI\]](#)
- [32] Guo J, Zhou B, Zong R et al. Stretchable and Highly Sensitive Optical Strain Sensors for Human-Activity Monitoring and Healthcare. *Acs Appl Mater Inter*, 2019; 11: 33589-33598.[\[DOI\]](#)
- [33] Dai M, Billoti E, Broer DJ et al. A Real Time Optical Strain Sensor Based on a Cholesteric Liquid Crystal Network. *RSC Adv*, 2013; 3: 18794-18798.[\[DOI\]](#)
- [34] Moghadam BH, Hasanzadeh M, Simchi A. Self-Powered Wearable Piezoelectric Sensors Based on Polymer Nanofiber-Metal-Organic Framework Nanoparticle Composites for Arterial Pulse Monitoring. *Acs Appl Nano Mater*, 2020; 3: 8742-8752.[\[DOI\]](#)
- [35] Zhu M, Chng S, Cai W et al. Piezoelectric polymer nanofibers for pressure sensors and their applications in human activity monitoring. *Rsc Adv*, 2020; 10: 21887-21894.[\[DOI\]](#)
- [36] Lu K, Huang W, Guo J et al. Ultra-sensitive strain sensor based on flexible poly (vinylidene fluoride) piezoelectric film. *Nanoscale Res Lett*, 2018; 13: 83.[\[DOI\]](#)
- [37] Heikenfeld J, Jajack A, Rogers J et al. Wearable sensors: modalities, challenges, and prospects. *Lab Chip*, 2018; 18: 217-248.[\[DOI\]](#)
- [38] Cheng L, Qian W, Wei L et al. A Highly Sensitive Piezoresistive Sensor with Interlocked Graphene Microarrays for Meticulous Monitoring of Human Motions. *J Mater Chem C*, 2020; 8: 11525-11531.[\[DOI\]](#)
- [39] Lu N, Lu C, Yang S et al. Highly Sensitive Skin-Mountable Strain Gauges Based Entirely on Elastomers. *Adv Funct Mater*, 2012; 22: 4044-4050.[\[DOI\]](#)
- [40] Lin Y, Liu S, Chen S et al. A highly stretchable and sensitive strain sensor based on graphene elastomer composites with a novel double-interconnected network. *J Mater Chem C*, 2016; 4: 6345-6352.[\[DOI\]](#)
- [41] Chen F, Gu Y, Cao S et al. Low-Cost Highly Sensitive Strain Sensors for Wearable Electronics. *J Mater Chem C*, 2017; 5: 10571-10577.[\[DOI\]](#)
- [42] Ryu S, Lee P, Chou J et al. Extremely Elastic Wearable Carbon Nanotube Fiber Strain Sensor for Monitoring of Human Motion. *Acs Nano*, 2015; 9: 5929-5936.[\[DOI\]](#)
- [43] Kim K, Lee J, Sim S et al. Patterned Carbon Nanotube Bundles as Stretchable Strain Sensors for Human Motion Detection. *Acs Appl Nano Mater*, 2020; 3: 11408-11415.[\[DOI\]](#)
- [44] Cai Y, Qin J, Li W et al. A stretchable, conformable, and biocompatible graphene strain sensor based on a structured

- hydrogel for clinical application. *J Mater Chem A*, 2019; 7: 27099-27109.[\[DOI\]](#)
- [45] Jiang Y, He Q, Cai J et al. Flexible Strain Sensor with Tunable Sensitivity via Microscale Electrical Breakdown in Graphene/Polyimide Thin Films. *Acs Appl Mater Inter*, 2020; 12: 58317-58325.[\[DOI\]](#)
- [46] Wang H, Zhou R, Li D et al. High-Performance Foam-Shaped Strain Sensor Based on Carbon Nanotubes and $\text{Ti}_3\text{C}_2\text{T}_x$ MXene for the Monitoring of Human Activities. *Acs Nano*, 2021; 15: 9690-9700.[\[DOI\]](#)
- [47] Shi X, Wang H, Xie X et al. Bioinspired Ultrasensitive and Stretchable MXene-Based Strain Sensor via Nacre-Mimetic Microscale “Brick-and-Mortar” Architecture. *Acs Nano*, 2019; 13: 649-659.[\[DOI\]](#)
- [48] Liu G, Yang F, Xu J et al. Ultrasonically Patterning Silver Nanowire-Acrylate Composite for Highly Sensitive and Transparent Strain Sensors Based on Parallel Cracks. *Acs Appl Mater Inter*, 2020; 12: 47729-47738.[\[DOI\]](#)
- [49] Liao X, Zhang Z, Kang Z et al. Ultrasensitive and Stretchable Resistive Strain Sensors Designed for Wearable Electronics. *Mater Horiz*, 2017; 4: 502-510.[\[DOI\]](#)
- [50] Su Y, Lin Y, Chang C et al. Gold Nanoparticle Thin Film-Based Strain Sensors for Monitoring Human Pulse. *Acs Appl Nano Mater*, 2021; 4: 1712-1718.[\[DOI\]](#)
- [51] Yang Y, Shi L, Cao Z et al. Strain Sensors with a High Sensitivity and a Wide Sensing Range Based on a $\text{Ti}_3\text{C}_2\text{T}_x$ (MXene) Nanoparticle-Nanosheet Hybrid Network. *Adv Funct Mater*, 2019; 29: 1807882.[\[DOI\]](#)
- [52] Sun J, Yuan Y, Lu G et al. A Transparent, Stretchable, Stable, Self-Adhesive Ionogel-Based Strain Sensor for Human Motion Monitoring. *J Mater Chem C*, 2019; 7: 11244-11250.[\[DOI\]](#)
- [53] Xiang S, Chen S, Yao M et al. Strain Sensor Based on a Flexible Polyimide Ionogel for Application in High- and Low-Temperature Environments. *J Mater Chem C*, 2019; 7: 9625-9632.[\[DOI\]](#)
- [54] Wu J, Wang H, Su Z et al. Highly Flexible and Sensitive Wearable E-Skin Based on Graphite Nanoplatelet and Polyurethane Nanocomposite Films in Mass Industry Production Available. *Acs Appl Mater Inter*, 2017; 9: 38745-38754.[\[DOI\]](#)
- [55] Zhang M, Wang C, Wang Q et al. Sheath-Core Graphite/Silk Fiber Made by Dry-Meyer-Rod-Coating for Wearable Strain Sensors. *Acs Appl Mater Inter*, 2016; 8: 20894-20899.[\[DOI\]](#)
- [56] Jinho L, Hyeyeon C, Hee C. Exfoliated Graphite Electrodes for Organic Single-Crystal Field-Effect Transistor Devices. *Acs Appl Electron Ma*, 2019; 1: 2174-2183.[\[DOI\]](#)
- [57] Chen Y, Hu S, Lin C et al. Graphite-based selectorless RRAM: improvable intrinsic nonlinearity for array applications. *Nanoscale*, 2018; 10: 15608-15614.[\[DOI\]](#)
- [58] Chen M, Wu G, Zhang M et al. A highly efficient nanographite electron transport layer for high performance ZnO/Si solar cells. *Sustain. Energy Fuel*, 2018; 2: 820-826.[\[DOI\]](#)
- [59] Chen J, Dong H, Zhang L et al. Graphitic carbon nitride doped SnO_2 enabling efficient perovskite solar cells with pces exceeding 22%. *J Mater Chem A*, 2020; 8: 2644-2653.[\[DOI\]](#)
- [60] Wu S, Li T, Tong Z et al. High-Performance Thermally Conductive Phase Change Composites by Large-Size Oriented Graphite Sheets for Scalable Thermal Energy Harvesting. *Adv Mater*, 2019; 31: 1905099.[\[DOI\]](#)
- [61] Li X, Wang Y, Chen B et al. Record high thermoelectric performance of expanded graphite/carbon fiber cement composites enhanced by ionic liquid 1-butyl-3-methylimidazolium bromide for building energy harvesting. *J Mater Chem C*, 2021; 9: 3682-3691.[\[DOI\]](#)
- [62] Zheng R, Yu H, Zhang X et al. A TiSe_2 -Graphite Dual Ion Battery: Fast Na-Ion Insertion and Excellent Stability. *Angew Chem Int Ed*, 2021; 60: 18430.[\[DOI\]](#)
- [63] Li L, Zhang W, Pan W et al. Application of expanded graphite-based materials for rechargeable batteries beyond lithium-ions. *Nanoscale*, 2021; 13: 19291-19305.[\[DOI\]](#)
- [64] Gao J, Wu L, Guo Z et al. A hierarchical carbon nanotube/ SiO_2 nanoparticle network induced superhydrophobic and conductive coating for wearable strain sensors with superior sensitivity and ultra-low detection limit. *J Mater Chem C*, 2019; 7: 4199-4209.[\[DOI\]](#)
- [65] Yang C, Zhang D, Wang D et al. Ultra-sensitive, stretchable, and bidirectional wearable strain sensor for human motion detection. *J Mater Chem C*, 2022; 10: 7076-7086.[\[DOI\]](#)
- [66] Kim Y, P. Kim M, Park J et al. Binary Spiky/Spherical Nanoparticle Films with Hierarchical Micro/Nanostructures for High-Performance Flexible Pressure Sensors. *Acs Appl Mater Inter*, 2020; 12: 58403-58411.[\[DOI\]](#)
- [67] Jeong C, Ko H, Kim H et al. Bioinspired, High-Sensitivity Mechanical Sensors Realized with Hexagonal Microcolumnar Arrays Coated with Ultrasonic-Sprayed Single-Walled Carbon Nanotubes. *Acs Appl Mater Inter*, 2020; 12: 18813-18822.[\[DOI\]](#)
- [68] Wu X, Surendran A, Moser M et al. Universal Spray-Deposition Process for Scalable, High-Performance, and Stable Organic Electrochemical Transistors. *Acs Appl Mater Inter*, 2020; 12: 20757-20764.[\[DOI\]](#)
- [69] Nishinaka M, Jinno H, Jimbo Y et al. High-Transconductance Organic Electrochemical Transistor Fabricated on Ultrathin Films Using Spray Coating. *Small Struct*, 2021; 2: 2000088.[\[DOI\]](#)
- [70] Chou L, Chan J, Liu C. Progress in Spray Coated Perovskite Films for Solar Cell Applications. *Sol RRL*, 2022; 6: 2101035.[\[DOI\]](#)
- [71] Cassella E, Spooner E, Thornber T et al. Gas-Assisted Spray Coating of Perovskite Solar Cells Incorporating Sprayed Self-Assembled Monolayers. *Adv Sci*, 2022; 9: 2270087.[\[DOI\]](#)
- [72] Carey T, Jones C, Deganello D et al. Spray-Coating Thin Films on Three-Dimensional Surfaces for a Semitransparent Capacitive-Touch Device. *Acs Appl Mater Inter*, 2018; 10: 19948-19956.[\[DOI\]](#)
- [73] Kang D, Pikhitsa P, Choi Y et al. Ultrasensitive mechanical crack-based sensor inspired by the spider sensory system. *Nature*, 2014; 516: 222-226.[\[DOI\]](#)
- [74] Lin M, Zheng Z, Yang L et al. A High-Performance, Sensitive, Wearable Multifunctional Sensor Based on Rubber/CNT for Human Motion and Skin Temperature Detection. *Adv Mater*, 2022; 34: 2107309.[\[DOI\]](#)
- [75] Pang C, Lee GY, Kim Ti et al. A flexible and highly sensitive strain-gauge sensor using reversible interlocking of nanofibres. *Nature Mater*, 2012; 11: 795-801.[\[DOI\]](#)
- [76] Niu S, Matsuhisa N, Beker L et al. A wireless body area sensor

- network based on stretchable passive tags. *Nat Electron*, 2019; 2: 361-368.[\[DOI\]](#)
- [77] Boutry C, Kaizawa Y, Schroeder B et al. A stretchable and biodegradable strain and pressure sensor for orthopaedic application. *Nat Electron*, 2018; 1: 314-321.[\[DOI\]](#)
- [78] Lee J, Ihle S, Pellegrino G et al. Stretchable and suturable fibre sensors for wireless monitoring of connective tissue strain. *Nat Electron*, 2021; 4: 291-301.[\[DOI\]](#)
- [79] Wang W, Wang S, Rastak R et al. Strain-insensitive intrinsically stretchable transistors and circuits. *Nat Electron*, 2021; 4: 143-150.[\[DOI\]](#)
- [80] Yong K, De S, Leem J et al. Kirigami-inspired strain-insensitive sensors based on atomically-thin materials. *Mater Today*, 2020; 34: 58-65.[\[DOI\]](#)
- [81] Pan S, Liu Z, Wang M et al. Mechanically Interlocked Hydrogel-Elastomer Hybrids for On-Skin Electronics. *Adv Mater*, 2019; 30: 1903130.[\[DOI\]](#)
- [82] Wu S, Peng S, Han Z et al. Ultrasensitive and stretchable strain sensors based on mazelike vertical graphene network. *Acs Appl Mater Inter*, 2018; 10: 36312.[\[DOI\]](#)
- [83] Gong S, Lai D, Su B et al. Highly Stretchy Black Gold E-Skin Nanopatches as Highly Sensitive Wearable Biomedical Sensors. *Adv Electron Mater*, 2015; 1: 1400063.[\[DOI\]](#)
- [84] Zheng Y, Li Y, Dai K et al. A highly stretchable and stable strain sensor based on hybrid carbon nanofillers/polydimethylsiloxane conductive composites for large human motions monitoring. *Compos Sci Technol*, 2018; 156: 276-286.[\[DOI\]](#)
- [85] Seyedin M, Razal J, Innis P et al. Strain-Responsive Polyurethane/PEDOT:PSS Elastomeric Composite Fibers with High Electrical Conductivity. *Adv Funct Mater*, 2014; 24: 2957-2966.[\[DOI\]](#)
- [86] Madhavan R. Epidermis-Like High Performance Wearable Strain Sensor for Full-Range Monitoring of the Human Activities. *Macromol Mater Eng*, 2022; 307: 2200034.[\[DOI\]](#)
- [87] Chen X, Zhang Z, Tao X et al. A novel double-sided fabric strain sensor array fabricated with a facile and cost-effective process. *Sensor Actuat A-Phys*, 2024; 370: 115208.[\[DOI\]](#)
- [88] Liu W, Huang Y, Peng Y et al. Stable Wearable Strain Sensors on Textiles by Direct Laser Writing of Graphene. *Acs Appl Nano Mater*, 2020; 3: 283-293.[\[DOI\]](#)
- [89] Yang Y, Shi L, Cao Z et al. Strain Sensors with a High Sensitivity and a Wide Sensing Range Based on a $\text{Ti}_3\text{C}_2\text{T}_x$ (MXene) Nanoparticle-Nanosheet Hybrid Network. *Adv Funct Mater*, 2019; 29: 1807882.[\[DOI\]](#)
- [90] Chen S, Wei Y, Lin Y et al. Ultrasensitive Cracking-Assisted Strain Sensors Based on Silver Nanowires/Graphene Hybrid Particles. *Acs Appl Mater Inter*, 2016; 8: 25563-25570.[\[DOI\]](#)
- [91] Aslanidis E, Skotadisa E, Tsoukalas D. Resistive crack-based nanoparticle strain sensors with extreme sensitivity and adjustable gauge factor, made on flexible substrates. *Nanoscale*, 2021; 13: 3263-3274.[\[DOI\]](#)
- [92] Han Z, Liu L, Zhang J et al. High-performance flexible strain sensor with bio-inspired crack arrays. *Nanoscale*, 2018; 10: 15178-15186.[\[DOI\]](#)
- [93] Kulyk B, Silvestre S, Martins R et al. Laser-Induced Graphene from Paper for Mechanical Sensing. *Acs Appl Mater Inter*, 2021; 13: 10210-10221.[\[DOI\]](#)
- [94] Liu J, Wang P, Li G et al. A highly stretchable and ultra-sensitive strain sensing fiber based on a porous core-network sheath configuration for wearable human motion detection. *Nanoscale*, 2022; 14: 12418-12430.[\[DOI\]](#)
- [95] Nankali M, Navidbakhsh M, Karimia M et al. Highly stretchable and sensitive strain sensors based on carbon nanotube-elastomer nanocomposites: the effect of environmental factors on strain sensing performance. *J Mater Chem C*, 2020; 8: 6185-6195.[\[DOI\]](#)
- [96] Kong W, Zhou C, Dai K et al. Highly stretchable and durable fibrous strain sensor with growth ring-like spiral structure for wearable electronics. *Compos Part B-Eng*, 2021; 225: 109275.[\[DOI\]](#)
- [97] Huang Q, Al-Milaji KN, Zhao H. Inkjet Printing of Silver Nanowires for Stretchable Heaters. *Acs Appl Nano Mater*, 2018; 1: 4528-4536.[\[DOI\]](#)
- [98] Cai G, Yang M, Xu Z et al. Flexible and wearable strain sensing fabrics. *Chem Eng J*, 2017; 325: 396-403.[\[DOI\]](#)
- [99] Lu Y, Liu Z, Yan H. Ultrastretchable Conductive Polymer Complex as a Strain Sensor with a Repeatable Autonomous Self-Healing Ability. *Acs Appl Mater Inter*, 2019; 11: 20453-20464.[\[DOI\]](#)
- [100] Wang R, Xu W, Shen W et al. A highly stretchable and transparent silver nanowire/thermoplastic polyurethane film strain sensor for human motion monitoring. *Inorg Chem Front*, 2019; 6: 3119-3124.[\[DOI\]](#)
- [101] Kong W, Zhou C, Li Z et al. A highly stretchable and stable strain sensor based on hybrid carbon nanofillers/polydimethylsiloxane conductive composites for large human motions monitoring. *Compos Sci Technol*, 2018; 156: 276-286.[\[DOI\]](#)
- [102] Park S, Ahn S, Sun J et al. Highly Bendable and Rotational Textile Structure with Prestrained Conductive Sewing Pattern for Human Joint Monitoring. *Adv Funct Mater*, 2019; 29: 1808369.[\[DOI\]](#)
- [103] Herbert R, Lim H, Yeo W. Printed, Soft, Nanostructured Strain Sensors for Monitoring of Structural Health and Human Physiology. *Acs Appl Mater Inter*, 2020; 12: 25020-25030.[\[DOI\]](#)